Talanta 81 (2010) 294–300

Contents lists available at ScienceDirect

Talanta

journal homepage: www.elsevier.com/locate/talanta

Remote gas sampling with a swirl air stream

Yuri N. Kolomiets*, Viktor V. Pervukhin

Nikolaev Institute of Inorganic Chemistry of SB RAS, Acad. Lavrentieva Ave. 3, 630090 Novosibirsk, Russia

ARTICLE INFO

Article history:
Received 26 May 2009
Received in revised form
20 November 2009
Accepted 29 November 2009
Available online 11 December 2009

Keywords:
Remote gas sampling
Swirl sampling stream
Vortex core
API-IMIS–MS

ABSTRACT

One of the promising techniques of remote gas sampling from the surface or from the inside of an object involves the use of a swirl air stream. The case in which a swirl sampling stream produces a vortex core of a composite swirl is of most interest. But a practical implementation of a vortex sampling faces major problems due to the fact that the majority of the available gas analyzers feature a low analytical flow. This offers limitations on sampling distance and reduced pressure created at the object surface. This paper deals with the problem of adjusting vortex and sampling flows for a mass-spectrometer with atmospheric pressure ionization used for remote sampling of diethylanyline vapors. It is shown experimentally that additional sampling flow (Q_{add}) that coaxially envelops an analytical channel allows one to achieve conditions required for the formation of a vortex core, which is characterized by an increased tangential component of the flow velocity at its boundary and abnormally low pressure on the core axis. A satisfactory agreement between the calculations by the composite vortex model and the experiment is obtained. The studies performed have shown that the optimal relationship between vortex (Q_{vortex}) and additional flows is $Q_{vortex}/Q_{add} = 1.3$ and is symbate in terms of both gas dynamic parameters (minimal diameter of a backflow core) and sampling efficiency. It is shown that both the sampling distance and sampling area depend mainly on geometric sampler parameters. The experiments performed have revealed the unique ability of a vortex sampling flow in the form of a composite vortex to focus the sample inside the vortex core, thus preventing its dilution over the backflow.

1. Introduction

In the gas analysis practice it is often required to take gas samples from the surface and from the inside of the object under study. This happens: in forensic science upon examination of material evidences from a crime site; in geology upon analysis of rock samples from different deposits; in medicine upon analysis of a gas liberation composition from a skin surface; in check portals of air ports for the detection of concealed explosives and drugs in luggage and hand-luggage. In many cases the use of contact sampling methods is rather complicated, since it requires more time, personnel, and there is a high probability that interference compounds will be introduced. The use of conventional aspiration sampling devices is inefficient owing to a small sampling area restricted by an inlet nozzle diameter. This makes sampling difficult since the objects under study are varied in forms, dimensions and configurations.

A sampler used for remote gas sampling from the surface and from the inside of an object should be able to: (a) remove air from the inside of the object; (b) transport vapors to the analyzer with minimal losses. We think that a vortex air stream is the best suited for this purpose. Unlike a straight flow, a vortex one features three velocity vector components: axial (V_c), radial (V_r) and tangential (V_f). An important parameter of the vortex flow is its swirl intensity that is determined by the swirl parameter $S = M/(KR)$, where K is the momentum of a stream, M is the angular momentum, and R is the nozzle radius [1]. Experimental studies show that the flow swirl has a pronounced effect on the stream spread, its size, form, flow stability and occurrence of recirculation areas [2–18]. Vortex flows have found practical use in cyclone combustion chambers, separators and vortex burners. A possibility to use a vortex stream in analytical chemistry for remote gas sampling was first disclosed in [19]. The following distinctive features of the vortex streams have attracted the author's attention. First, static pressure over the entire vortex flow volume is below atmospheric pressure due to the centrifugal stream dispersion and changes both in radial and in axial directions. Second, with a high swirl intensity, when $S > 0.5$, an axial velocity vector in a paraxial region reverses sign, and a backflow is produced. For remote sampling it is suggested to blow an object with the vortex flow with high swirl intensity so that the entire object or a part of it is found to be in the backflow area. Impurity vapors taken from the surface or removed from the inside of the object by a reduced pressure of the vortex stream are trapped by the backflow and transported to a stream head where an inlet nozzle of a gas analyzer or a concentrator is placed. It should be mentioned therewith that the structure of the vortex flow itself enhances sampling efficiency. It is shown in [20] that with a moderate or high stream

* Corresponding author. Fax: +7 383 330 94 89.
E-mail address: ykolom@che.nsk.su (Y.N. Kolomiets).

0039-9140/$ – see front matter © 2009 Elsevier B.V. All rights reserved.
doi:10.1016/j.talanta.2009.11.071

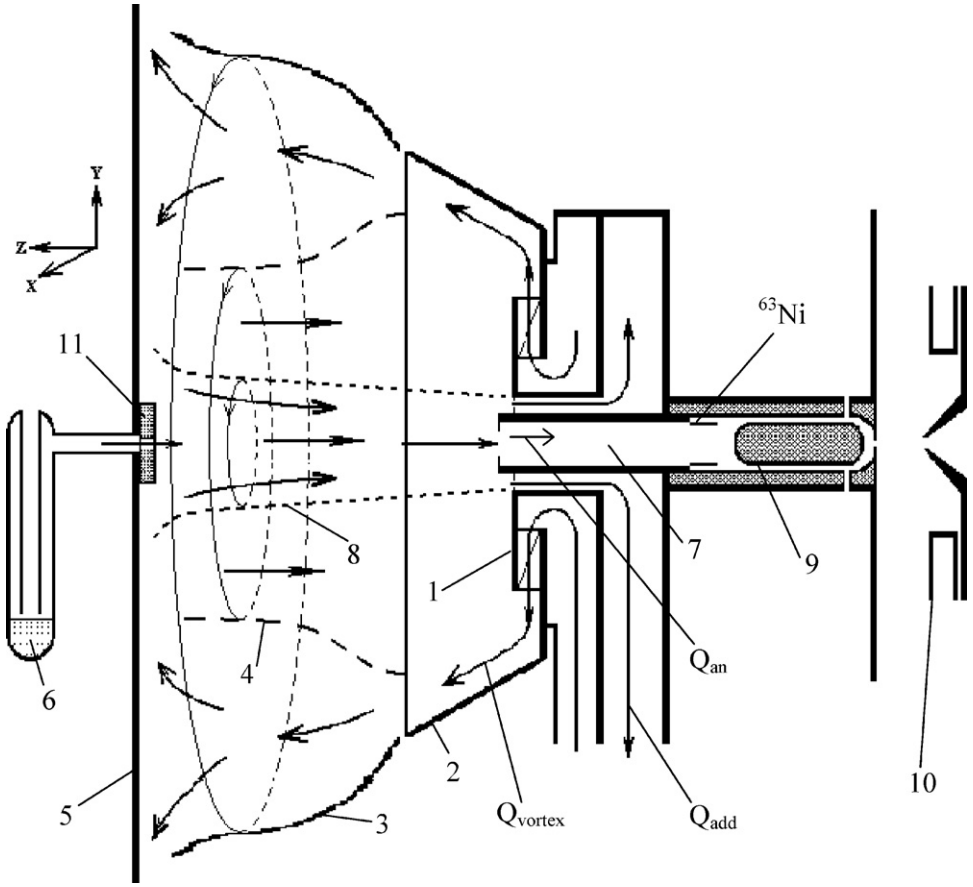

Fig. 1. Scheme of the experiment with the vortex sampler provided with additional flow (model II). 1 – fixed impeller, 2 – reflector, 3 – vortex stream boundary, 4 – backflow boundary, 5 – screen, 6 – glass vessel with test compound, 7 – analytical channel, 8 – vortex core boundary, 9 – IMIS separation channel, 10 – MS inlet stage, 11 – replaceable membrane.

swirl radial velocity is directed to the both sides from a maximum of an axial velocity component. As a result, sample vapors removed from the inside of the object or trapped from its surface during their transportation by the backflow shift to the flow axis, which reduces sample dilution and enhances sample injection into the analyzer.

The case in which a vortex stream is produced by a swirl fan flow and is completely overlapped by an object surface holds the greatest interest for the remote sampling with a vortex stream [21]. Such a sampling technique is represented schematically in Fig. 1. Flow Q_{vortex} with a centrifugal pump (not shown) is fed to fixed impeller (1) with an angle of blade of 45° and creates a vortex fan stream that spreads over the inside surface of reflector (2) producing a volumetric vortex flow along the reflector axis towards the object. The boundaries of direct and backflows are shown by solid (3) and dashed (4) lines. Reduced pressure produced by the vortex flow removes sample vapors from an opening in the object envelope; therewith the sample via the backflow is transported to a stream head. Sample vapors from the backflow are fed into the gas analyzer. When the conditions $Q_{out} \sim Q_{cf}$ and $X \leq D$ (where Q_{out} is the flow removed from the backflow, Q_{cf} is the backflow rate, X is the distance from the object surface to the reflector, D is the reflector diameter) are met, a gas dynamic structure of such a vortex backflow presents a composite vortex which is a mixture of forced and free ones [22].

A forced vortex or a vortex core with the radius independent of increased angular rotation velocity is localized close to the axis (dotted line 8 in Fig. 1) and has a radius corresponding to that of the inlet nozzle of the sampling channel. A free (or a potential) vortex, whose angular velocity is inversely proportional to the square of the radius ($\omega \sim 1/r^2$), occupies the rest body of the backflow. With $Q_{out} \sim Q_{cf}$ the dependence of pressure and angular rotation velocity on the radius in different regions of the vortex sampling stream can be expressed by equation [21]:

$$P(r) = P_{atm} - \frac{\rho V_{fR}^2}{2} + \frac{\rho\omega_1^2}{2}(r^2) \quad (r_1 < r < R) \tag{1}$$

$$\omega = \omega_1 \quad (r_1 < r < R) \tag{2}$$

$$P(r) = P_{atm} - \frac{\rho V_{fR}^2}{2} + \frac{\rho\omega_1^2 r_1^2}{2}\left(2 - \left(\frac{r_1}{r}\right)^2\right) \quad (r_2 < r < r_1) \tag{3}$$

$$\omega = \omega_1\left(\frac{r_1}{r}\right)^2 \quad (r_2 < r < r_1) \tag{4}$$

$$P(r) = P_{atm} - \frac{\rho V_{fR}^2}{2} + \frac{\rho\omega_1^2 r_1^2}{2}\left(2 - \left(\frac{r_1}{r}\right)^2 - \left(\frac{r_1}{r_2}\right)^4 \frac{r_2^2 - r^2}{r_1^2}\right) \quad (0 < r < r_2) \tag{5}$$

$$\omega = \omega_1\left(\frac{r_1}{r_2}\right)^2 \quad (0 < r < r_2) \tag{6}$$

where P_{atm} is the atmospheric pressure, r_1 is the radius of the backflow, r_2 is the radius of the sampling channel inlet nozzle, ω_1 is the angular rotation velocity of the stream with $r > r_1$, R is the reflector radius, V_{fR} is the tangential velocity with $r = R$, ρ is the air density.

As it is shown in paper [21] the composite vortex is mostly suited for remote sampling, since it exhibits low sample dilution and loss upon transportation due to a higher sample concentration by a radial flow close to the stream axis and a possibility to create

marked reduced pressure, with the diameter of the vortex stream being relatively small. But the practical use of the vortex sampler faces problems due to the fact that the majority of available gas analyzers feature a rather low analytical flow rate (Q_{an}). This imposes limitations on sampling distance and reduced pressure created at the object surface.

To avoid this it is suggested to use an additional channel that coaxially envelops the analytical channel and allows one to increase the flow removed from the backflow to desired values. Such a sampling technique is shown in Fig. 1. Additional flow (Q_{add}) allows one to increase the vortex flow rate leaving its structure unchanged, thus increasing sampling distance and reduced pressure in the sampling stream. But it is unknown how great sample losses will be. This is of particular importance for a relationship between the flows $Q_{add} \gg Q_{an}$, when much of the sample can leave with additional flow, is not analyzed, provided that the concentration of the sample near the stream axis turns to be inefficient. In available vortex sampler designs [23,24] and vortex samplers developed for drift spectrometric (MO-2 ("SIBEL", Russia), Pilot-M ("LAVANDA-U", Russia)) and gas chromatographic (ECHO-M, ECHO-EW ("MULTICHROM", Russia)) analyzers no due consideration is given for the problems of adjusting vortex and sampling flow, and we have no information on the papers covering these problems.

This paper deals with the problems of vortex and sampling flow adjustment upon vortex sampling. We used a mass-spectrometer as a gas analyzer with atmospheric pressure ionization (MS) in tandem with an ion mobility increment spectrometer (IMIS). To determine optimal modes of the vortex sampler operation, we studied the dependence of gas dynamic parameters of the vortex sampling stream (reduced pressure, tangential velocity, radial distribution of these parameters over the vortex sampling stream) and remote sampling efficiency on the relationship between vortex, additional and analytical flows.

2. Experimental

2.1. Instrumentation

For experiments we used two models of the vortex sampler. The main device parameters are given in Table 1. In the sampler (model I) an additional channel is missing, and the sample by analytical flow ($Q_{out} = Q_{an}$) is removed from the backflow. The sampler (model II) is provided with an additional channel that coaxially envelops the analytical channel. The sample is removed from the backflow with analytical and additional flows ($Q_{out} = Q_{add} + Q_{an}$) simultaneously. The reflector diameter is chosen so that the ratio between it and the diameter of the outlet channel is 5:1. (The outlet channel is presented by the analytical channel in model I and by an additional one in model II.)

The design of the vortex sampler (model II) allows one to change flows Q_{vortex} and Q_{add} independently of each other. The range of flow rate variations is given in Table 1.

We used a mass-spectrometer as a gas analyzer with atmospheric pressure ionization (MS API) and preliminary ion separation by an ion mobility increment spectrometer (IMIS). The mass-spectrometer with atmospheric pressure ionization developed on the basis of a MX-7304 mass-analyzer was described in detail in [25]. The IMIS design and its interface with the MS are similar to those described in [26]. The IMIS separation gap is a coaxial cylindrical channel with 60 mm in length provided with central and external electrodes 8.8 mm and 12 mm in diameter, respectively. At exit the separation cylindrical channel slips into a hemispherical channel provided with an outlet of 0.3 mm in diameter, which is an inlet to the MS. In all of the experiments with the IMIS–MS tandem the analytical flow was $Q_{an} = 35\ cm^3/s$. We used a radioactive ^{63}Ni source with an activity of 10 mCi (Izotop Saint-Petersburg, Russia) to ionize the sample. The source was placed in an ionization chamber, with a cylindrical cavity of 13 mm in diameter and 10 mm in length, in front of the separation gap.

The scheme of experiment performed with the vortex sampler with additional flow (model II) is given in Fig. 1. Only the IMIS separation gap and the MS inlet stage are shown on the part of the gas analyzer. We used screen (5) with an opening in the center, as an object model. The screen was made of acrylic plastic of 250 mm × 250 mm in size with an opening in the center to which open glass vessel (6) with saturated vapors of a test compound was connected. Reduced pressure created by the vortex flow removes test compound vapors from the vessel, and then the gas sample is transported by the backflow from the object to the stream head. In the vortex sampler of model II flow Q_{out} removed from the backflow is constituted by analytical (Q_{an}) and additional (Q_{add}) flows, whereas in model I it is equal to analytical flow Q_{an}. Sample vapors from the vortex core are fed into channel (7) of the API-IMIS–MS analyzer with analytical flow Q_{an}. Following β-source ionization, sample ions are first separated by mobility nonlinearity in the IMIS separation gap between the coaxial central and external electrodes, and thereafter they are additionally separated by the mass-spectrometer by the ratio of mass to charge (m/z). Such a dual separation allows one to reduce chemical background upon target compound detection.

To study sampling efficiency versus the position of the test compound vapor source, provision is made for axis positioning of the screen in X, Y, Z directions. (X and Y are the direction in the plane of the screen; Z is direction along the stream axis at right angle to the screen plane.) To determine the efficiency of sample removal from the inside of the object, we changed the diameter of the vapor source outlet from 2 mm to 0.3 mm. To do this, we attached removable membranes with an opening of a different diameter (Fig. 1(11)) to the place where test compound vapors emitted.

We determined the value of reduced pressure in the vortex sampling stream with an accuracy of ±0.7 Pa by a U-shaped inclined manometer with ethanol with an inclination of 10°. We measured tangential and axial velocities of the vortex sampling flow with an accuracy of ±0.02 m/s by the DISA 55M System Constant-temperature Anemometer of Disa Elektronik A/S, Denmark.

Table 1
Main parameters of vortex samplers.

Parameter	Model I	Model II
Reflector diameter, D_R, mm	44	100
Diameter of fixed vortex impeller, mm	25	58
Width of fixed vortex impeller, mm	3	5
Diameter of analytical channel, mm	9	13
Diameter of additional channel, mm	–	21
Range of vortex flow rate through fixed impeller, Q_{vortex}, cm^3/s	80–990	270–9000
Range of additional flow rate, Q_{add}, cm^3/s	–	80–3900
Analytical flow rate, Q_{an}, cm^3/s	35	35

2.2. Chemicals

For studies it was necessary to choose a compound possessing a rather high vapor pressure (to obtain sufficient sample), low adsorption capacity (to reduce the "residual memory" effect after signal registration), high proton affinity (for reliable registration by an API-mass-spectrometer). Thus, as a test compound we have chosen *N*,*N*-Diethylanyline (DEA) ($C_6H_5N(C_2H_5)_2$, molecular mass (*M*), 149 AMU) producing a peak with 150 AMU corresponding to a $(M+H)^+$ ion well separated from the background and registered with a high sensitivity. *N*,*N*-Diethylanyline (extra pure) was provided by LLC "Ekos", Moscow. The sample was subjected to flash distillation before use to remove impurities produced by oxidation during its storage. The IMIS parameters (voltage amplitude of asymmetric waveform voltage generator and compensation voltage) correspond to the optimal values required for DEA ions to pass through IMIS.

3. Results and discussion

The results obtained can be divided into two parts.

The first part of the results concerns determination of an optimal relationship between the vortex sampler flows. Vortex core with a minimal diameter produced in the sampling stream, on the one hand, and the maximum intensity of the signal registered, on the other hand, serve as criteria of the flow adjustment. To clarify this, we determined the dependence of the IMIS signal, reduced pressure ($P - P_{atm}$) and tangential velocity (V_f) on the rates of vortex and additional flows. We determined distribution of ($P - P_{atm}$) and (V_f) across the stream cross-section as well. Besides, we compared the results of gas dynamic measurements with calculations by the composite vortex model (expressions (1)–(6)). Therewith, we took into consideration reduction in core forming region, with additional and analytical flow rates being low ($Q_{an} + Q_{add} < Q_{cf}$) and empirical dependence for backflow Q_{cf} [21]:

$$Q_{cf} = 1.2Q_{vortex} \quad (7)$$

$$D_{cf} = 0.64D \quad (8)$$

where D_{cf} is an average diameter of a backflow.

The second part of the results concerns determination of the vortex sampling efficiency, ability of remote sample removal from an object. We determined the dependence of the IMIS–MS signal on the distance between the sampler and the object, on the amount by which the point of DEA vapor emission is displaced from the sampler axis, and on the cross-sectional area of the outlet channel for DEA vapors. The flow rates of the vortex samplers correspond to the optimal one.

3.1. Determination of optimum relationship between the vortex sampler flows

The most sensitive gas dynamic parameter characterizing the formation of vortex core in the sampling stream is the distribution of tangential velocity component (V_f) along the flow radius. In the familiar swirl stream its angular velocity is radius independent (except the stream boundary) and $V_f(r)$ is a linear function. Upon composite vortex formation, linearity $V_f(r)$ is violated. In this case, keeping with dependence $\omega(r)$ (4) and (6), V_f reaches a maximum at the boundary of vortex core [21]. Fig. 2 shows for two sampler models how tangential velocity of the vortex sampling stream is distributed along the flow radius. We placed the object screen and the probe of the anemometer at a distance of reflector radius (*R*) and 0.5*R*, respectively. The radius dependence is given in relative units for convenience. Flow rates Q_{vortex} and Q_{ad} are given in the legend to the drawing.

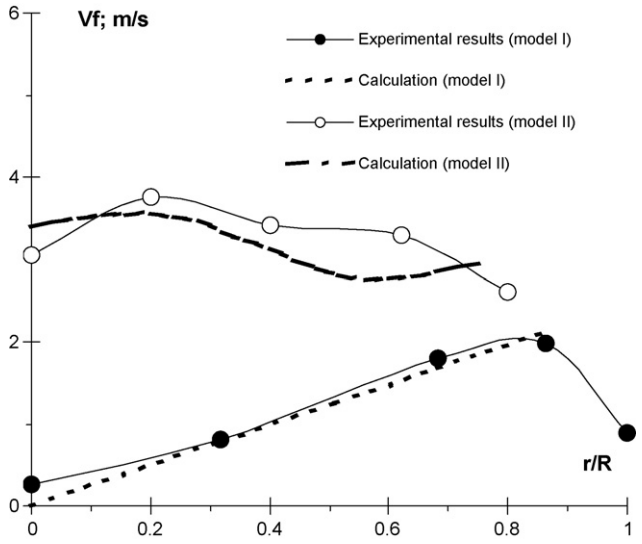

Fig. 2. Distribution of tangential velocity of the vortex stream along radius. Model I – sampler without additional flow, Q_{vortex} = 340 ml/s; model II – sampler with additional flow, Q_{vortex} = 4800 ml/s, Q_{ad} = 3750 ml/s, *R* – reflector radius.

As it is evident from Fig. 2, V_f in the sampler, model I (Fig. 2, solid line, black points) with $r/R < 0.85$ linearly depends on the radius and approaches zero near the stream axis. This corresponds to a conventional vortex stream with a constant angular velocity that represents a forced vortex. A dashed line shows the calculation of this dependence by the forced vortex model in the range $0 < r/R < 0.85$, which agrees well with experiment. A sharp loss in $V_f(r)$ values is observed during experiment with $r/R > 0.85$, this is evidently caused by the reduction of the vortex flow rotation by the environment. A vortex stream region for $r/R > 0.85$ is not considered in the model. As for the sampler, model II (Fig. 2, solid line, weight points) the experiment shows that tangential velocity, V_f, grows with the decreased radius, reaches maximum with $r/R \sim 0.2$ and then slightly decreases to the stream axis. The fact that V_f increases with decreased radius suggests that a composite vortex is produced in the stream which changes from the potential vortex into the forced one near the axis. By the composite vortex model tangential velocity on the stream axis should be zero. But we do not observe this in the experiment. This can be explained by a high mobility velocity of the vortex core whose axis constantly shifts over the object surface and affects the time-averaged experimental V_f values. In the model calculations we tried to take into account spatial fluctuations of the vortex core. The calculation data are shown by a dashed line approaching the experiment in the range $r/R < 0.4$. Qualitative and quantitative distinctions between the experiment and calculations for the sampler, model II are likely to be due to the random nature of the vortex core spatial fluctuations and difficulties by considering this in the model representation of the process.

It should be mentioned that linearity $V_f(r/R)$ for the sampler (model I) holds true for all values of Q_{vortex} up to 990 ml/s. This is due to a small area of the vortex core formation by a small analytical flow. The formation of a steady vortex stream in the sampler (model I) begins with Q_{vortex} = 210 ml/s, to which backflow Q_{cf} = 250 ml/s corresponds. In such a backflow with analytical flow Q_{an} = 35 ml/s, the diameter of the area of the vortex core formation is 10 mm. This corresponds to the analytical channel diameter (D_{an} = 9 mm, see Table 1). Vortex core is not produced under similar conditions for all values of $Q_{vortex} \geq 210$ ml/s, and the entire region of the vortex sampling flow represents a forced vortex with constant angular velocity. In the sampler (model I) with no composite vortex in the sampling stream, the main parameter of the flow adjustment (vortex Q_{vortex} and analytical Q_{an}) is a maximum

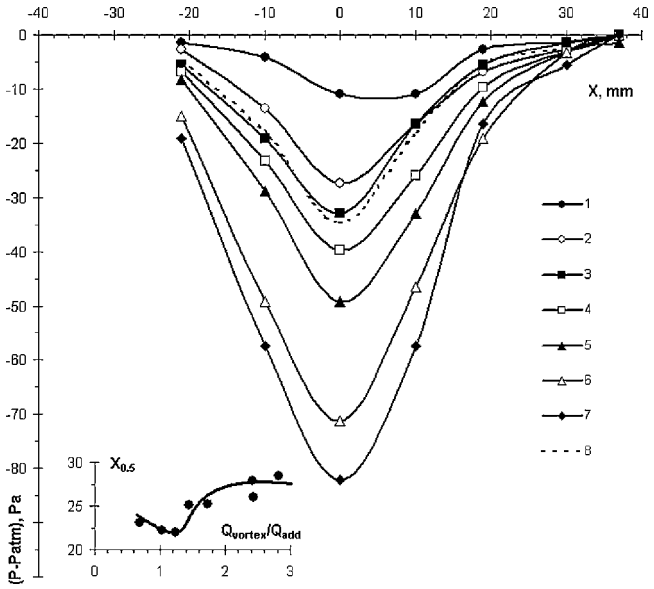

Fig. 3. Distribution of reduced pressure over cross-section of the vortex sampling stream versus Q_{vortex} for the vortex sampler (model II). 1 – Q_{vortex} = 2000 ml/s, 2 – Q_{vortex} = 3000 ml/s, 3 – Q_{vortex} = 3600 ml/s, 4 – Q_{vortex} = 4200 ml/s, 5 – Q_{vortex} = 5000 ml/s, 6 – Q_{vortex} = 7000 ml/s, 7 – Q_{vortex} = 8200 ml/s, 8 – calculation by the composite vortex model for Q_{vortex} = 3600 ml/s. X – coordinate in the stream radius direction. $X_{0.5}$ – half-width of reduced pressure peak. Distance between the reflector and object, 70 mm. Q_{add} = 2900 ml/s.

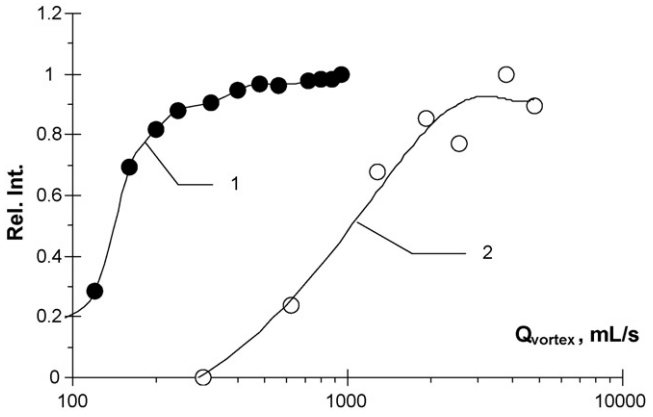

Fig. 4. DEA signal versus vortex flow. 1 – vortex sampler (model I), 2 – vortex sampler (model II).

reached by the IMIS–MS signal. As for the sampler (model II), the situation is more complicated, since three flows Q_{an}, Q_{vortex} and Q_{add} should be adjusted. Therefore, we first determined the best relationship between flows Q_{vorte} and Q_{add} defining reduced pressure $P - P_{atm}$ distribution in the cross-sectional area of the sampling stream for different values of the vortex and additional flows. With optimum relationship between Q_{vortex} and Q_{add} the half-width of $P - P_{atm}(X)$ dependence (X is coordinate in the stream radius direction) has a minimum, complying with a minimal vortex core diameter. Thereafter, we determined the agreement of flows Q_{an} and Q_{vortex} when the IMIS–MS signal reached a maximum, keeping relationship between Q_{vortex} and Q_{add} optimal.

Fig. 3 (the main graph) gives the X dependence of reduced pressure $(P - P_{atm})$ for model II for different values of relationship Q_{vortex}/Q_{add} (P is the static pressure in the sampling stream, P_{atm} is the atmospheric pressure). We changed relationship Q_{vortex}/Q_{add} varying vortex flow Q_{vortex} with constant additional flow Q_{add} = 2900 ml/s. As it is evident from the graph, a considerable increase in reduced pressure is observed near the axis for all values Q_{vortex}. The value of reduced pressure increases with the vortex flow and reaches −80 Pa with Q_{vortex} = 8200 ml/s. Therewith, the relationship between reduced pressure at the stream axis and the backflow boundary (X ~ 32 mm) ranges from 5 to 10, whereas in the familiar vortex flow presenting a forced vortex this parameter does not exceed 1.3. Such a growth of reduced pressure near the axis indicates that a composite vortex is produced in the sampling stream. If we plot the half peak width of reduced pressure ($X_{0.5}$ is peak width at its half height) versus relationship Q_{vortex}/Q_{add} (included graph of Fig. 2), we will see a minimum corresponding to a value of Q_{vortex}/Q_{add} = 1.3 on the curve obtained (on the main graph of Fig. 3, curve 3 with Q_{vortex} = 3600 ml/s corresponds this). The vortex core produced has a minimal diameter, which creates the most favorable conditions of the composite vortex with minor sample losses. Along with gas dynamic measurements we determined DEA signal registered by the IMIS–MS versus relationship between Q_{vorte} and $Q_{add.}$ We kept vortex flow Q_{vortex} constant equal to 1280 ml/s and varied additional flow Q_{add} from 0 to 3800 ml/s. Data are not given, but in the Q_{add} dependence of the signal intensity a well-defined peak with Q_{add} = 1000 ml/s is observed. Therewith, the relationship between the vortex and additional flows takes a value of Q_{vortex}/Q_{add} = 1.28, which is approaching the value obtained upon gas dynamic measurements. Hence, the relationship between the vortex and additional flows Q_{vortex}/Q_{add} = 1.3 is optimal for the sampler (model II), for which with a model of composite vortex [21] we determined distribution of reduced pressure $(P - P_{atm})$ in the cross-sectional area of the vortex stream (calculation is given by dashed line 8 in Fig. 3). Satisfactory agreement between calculations and experiments suggests that the model considered is applicable for the sample stream formation.

Fig. 4 shows DEA signal versus vortex flow rate for two sampler models. We placed the source outlet on the stream axis. The distance from the reflector to the object was 20 mm for model I, and 70 mm for model II. When measuring Q_{vortex} in model II, we kept constant relationship Q_{vortex}/Q_{add} = 1.3.

As Q_{vortex} in the sampler (model I) (Fig. 4, curve 1) increases, a sharp signal increase (up to Q_{vortex} = 240 ml/s) is observed, which thereupon smoothly transforms to its saturation. The region of the steady vortex stream formation causes the initial sharp increase in signal. With insignificant vortex flow (Q_{vortex} < 210 ml/s) linear stream velocity turns to be less than 1 m/s, which is comparable to convective flows in laboratory. This results in a marked tailing of the flow structure and considerable sample losses. As Q_{vortex} increases (Q_{vortex} > 240 ml/s), linear velocity exceeds 1 m/s, and the sampling flow becomes resistant to convection effects. Two processes affect the signal value in a region of Q_{vortex} > 240 ml/s. On the one hand, reduced pressure increases with the vortex flow resulting in an increase of the sample volume that enters the backflow from the object. On the other hand, the backflow increases with the vortex flow which under the forced vortex conditions tends to increase sample dilution and decrease the sample volume injected into the gas analyzer, since only a portion of the backflow enters the analytical flow. When Q_{vortex} reaches 480 ml/s, the signal registered becomes almost constant, and one may speak about the balance of these two processes. Hence, a value of Q_{vortex} = 480 ml/s is the best for this vortex sampler design. It is this value we use in the following experiments, unless otherwise specified.

In the sampler of model II (Fig. 4, curve 2) the signal increases with vortex flow Q_{vortex} and becomes saturated when Q_{vortex} = 2600 ml/s. No signal increase is observed with the further increase of the vortex flow to 5000 ml/s. Most likely, signal saturation is associated with a decrease in relationship Q_{an}/Q_{add}. One can conclude by the data obtained that flow rates Q_{vortex} = 2600 ml/s and Q_{add} = 2000 ml/s (with relationship Q_{vortex}/Q_{add} = 1.3) are the best to conduct experiments on remote sampling with the sampler (model

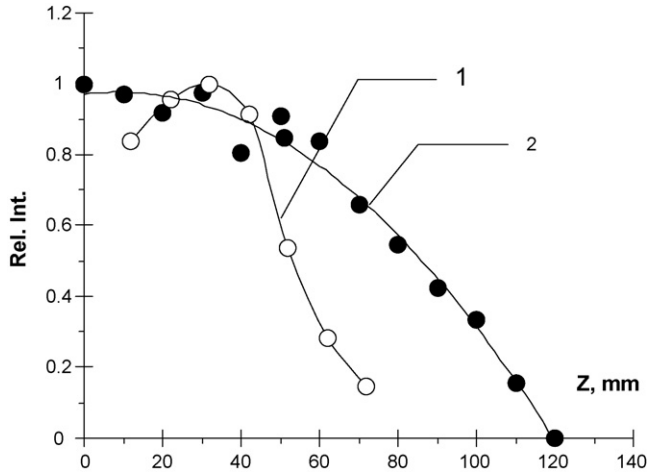

Fig. 5. DEA signal intensity versus distance between the reflector and object. The source is on the sampler axis. 1 – vortex sampler (model I), 2 – vortex sampler (model II).

II). In further experiments we use this relationship between the vortex and additional flows.

3.2. Research on the efficiency of remote vortex sampling

To evaluate the efficiency of remote sampling, we determined the dependence of the IMIS–MS signal on the distance to the object, on the value by which the point of DEA vapor emission is displaced relative to the sampler axis and on the cross-sectional area of the outlet channel for DEA vapors. The flow rates determined correspond to the optimal values. These measurements allow one to evaluate the feasibility of the vortex samplers, sampling distance, diameter of the sampling area and ability to remove samples through the opening in the object envelop.

Fig. 5 shows DEA signal intensity versus distance to the object screen for samplers of two models. As it is evident from Fig. 5, the sampler (model II) with a bigger reflector possesses a larger sampling distance. An increase of the reflector by a factor of 2.3 (from 44 mm to 100 mm) made it possible to increase sampling distance 1.5 times (from 70 mm to 110 mm). This corresponds to the reduction in the signal registered by a factor of 6.7 (from 1 to 0.15). One should mention that in model II the drop in signal begins with the distances much less than the reflector diameter (about 0.5*D*), thereafter the signal smoothly reduces to zero at a distance of 1.2*D*. In the sampler (model I) the signal remains almost unchanged to the distances corresponding to the reflector diameter (44 mm), and with a further increase in *Z* a sharper signal drop is observed than it is in the sampler (model II). Such different behaviors of the signal dependence on the sampling distance is likely to be connected with a different structure of the vortex sampling stream formed by the samplers.

Fig. 6 shows DEA signal intensity versus radial source displacement relative to the stream axis. The distance between the reflector and the object screen of the sampler (model I) and the sampler (model II) was 35 mm and 60 mm, respectively. As it is evident from Fig. 6 a sharp drop in signal upon the source displacement from the stream axis is observed for both samplers. It should be mentioned that reduced pressure behaves itself in the similar way (see Fig. 3), which is the chief cause of the related signal behavior. It is evident from the data obtained that effective diameter of model I and model II is 25 and 60 mm, respectively. In both cases this makes about 60% of the reflector diameter. It should be pointed out that the dependencies obtained are asymmetrical. This suggests that the fixed impeller creates the asymmetric vortex sampling flow.

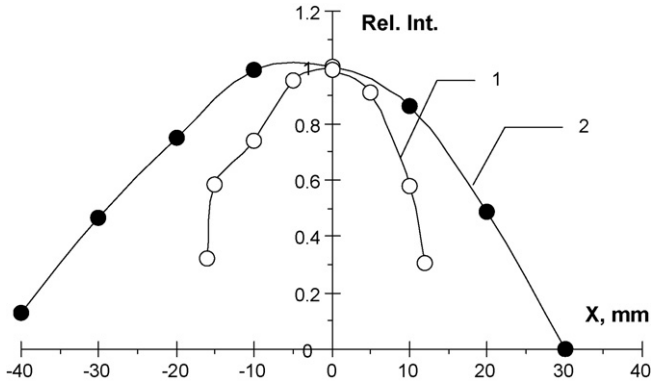

Fig. 6. DEA signal intensity versus radial source displacement relative to the stream axis. 1 – vortex sampler (model I), 2 – vortex sampler (model II).

The possibility for remote sample removal from the inside of the object through a small opening is a unique property of remote sampling. Indeed, a low-pressure area in the vortex flow suggests removal of the sample that is outside the action of the vortex stream followed by its transportation to the gas analyzer. It should be recognized that a higher reduced pressure suggests a more efficient sample removal. But a higher reduced pressure can yield losses of a target compound upon further sample transportation.

Fig. 7 showing the signal intensity of protonated diethylanyline versus the area of the opening, through which the sample is removed, can illustrate this. The distance between the reflector and the object screen was 35 mm for model I, and 70 mm for model II. It should be noted that the vortex sampler (model I) revealed a very high efficiency upon sample removal from within the object. As it is evident from Fig. 7, the signal intensity did not decrease as the area of the sample outlet reduced from 4 mm^2 to 0.25 mm^2. A sharp decrease in signal is observed for the outlet of 0.1 mm^2. In the sampler (model II) the signal steadily reduces over the entire range of area variations from 4 mm^2 to 0.25 mm^2, therewith decreasing by 40%. This is evidently caused by high sample losses during its transportation and trapping in the analytical channel of the analyzer.

The main research results are given in Table 2.

It should be emphasized that in the vortex sampler with additional flow a degree of sample dilution turned to be less than relationship Q_{add}/Q_{an} whose values run up to 107 in the experiments. Despite this relationship between the flows, we did manage to obtain a signal from the sample removed from the object. This

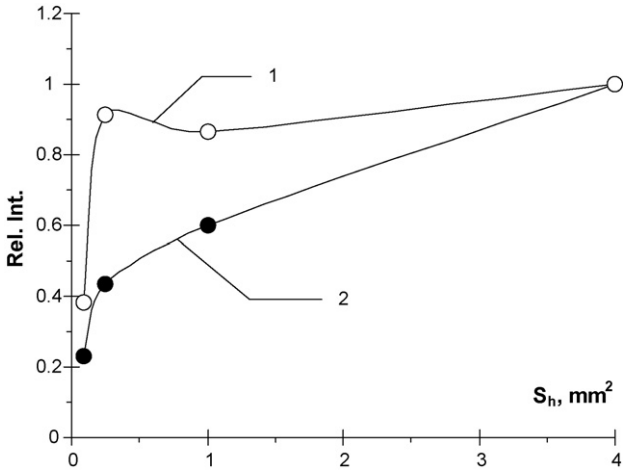

Fig. 7. DEA signal intensity versus cross-sectional area of the source channel. 1 – vortex sampler (model I), 2 – vortex sampler (model II). S_h – cross-sectional area of the source outlet.

Table 2
The main parameters of remote sampling efficiency of vortex samplers.

Parameter	Model I	Model II
Reflector diameter, D_R, mm	44	100
Optimal vortex flow rate, Q_{vortex}, cm^3/s	480	2600
Optimal relationship among Q_{vortex} and Q_{add}	–	$Q_{vortex}/Q_{add} = 1.3$
Maximum reduced pressure	−20 Pa at 20 mm from the source	−100 Pa at 70 mm from the source
Maximum sampling distance, mm	70–80	120
Optimal sampling distance, mm	30	70
Maximum sampling area, mm^2	620	3850

is due to the unique ability of the sampling vortex flow formed as a composite vortex to focus sample on the sampling flow axis at the center of the vortex core, and thus to prevent sampling dilution over the entire backflow.

4. Conclusion

Studies performed have shown that additional sampling flow Q_{add} that coaxially envelops the analytical channel allows one to achieve the conditions for the formation of a well-defined vortex core which is characterized by an increased tangential component of the flow velocity at its boundary and abnormally low pressure at the core axis. Satisfactory agreement between the composite vortex model calculations and experiments suggests that the model considered can be applied to the vortex stream formed.

Studies have shown that the optimal relationship between the vortex and additional flows $Q_{vortex}/Q_{add} = 1.3$ is symbate, with respect to both gas dynamic parameters (minimal diameter of the backflow core) and sampling efficiency.

A comparison between the remote sampling with the swirl stream applied in the systems with additional flow or without it has shown that both the sampling distance and sampling area depend on geometric sampler parameters. Unique ability of the vortex sampling stream formed as a composite vortex (the sampler with additional flow) to focus sample inside of the vortex core, preventing thus its dilution over the entire backflow, reveals therewith.

The results obtained indicate that vortex samplers with additional flow hold promise for remote gas sampling from unsealed objects.

The research results described in the paper were obtained with *N*,*N*-diethylamine that possesses a rather high saturated vapor pressure. But a research into the possibility of remote vortex gas sampling of low volatile compounds as explosives and drugs is of practical interest, and is an object of further investigations.

Acknowledgements

This work was supported by the Presidium of the Russian Academy of Sciences, grant no. 20.5-09 and partly by the Russian Foundation for Basic Research, project no. 07-08-00143-a.

References

[1] R.B. Akhmedov, Energy (1977) 18, Moscow (in Russian).
[2] A. Stambuleanu, Flame Combustion in Industry, Abacus Press, Tunbridge Wells, England, 1976.
[3] A.K. Gupta, D.G. Lilley, Flow Field Modeling and Diagnostics, Abacus Press, Tunbridge Wells, England, 1983.
[4] J.M. Beer, N.A. Chigier, Combustion Aerodynamics, Applied Science Publishers Ltd./Halsted-Wiley, London/New York, 1972.
[5] A.M. Kanury, Introduction to Combustion Phenomena, Gordon and Breach, New York, 1975.
[6] D.G. Lilley, AIAA J. 15 (August (8)) (1977) 1063.
[7] N. Syred, J.M. Beer, Combust. Flame 23 (1974) 143.
[8] A.A. Putnam, Flame Res. Commun. 18 (January) (1967).
[9] J.M. Beer, J. Inst. Fuel 45 (July) (1972) 370.
[10] D.B. Spalding, J. Inst. Fuel 44 (April) (1971) 196.
[11] N.A. Chigier, A. Chervinsky, Trans. ASME Series E., J. Appl. Mech. 34 (1967) 443.
[12] N.A. Chigier, J.M. Beer, J. Basic Eng. 86 (December (4)) (1964) 788.
[13] S.A. Beltagui, N.R.L. Maccallum, J. Inst. Fuel 49 (1976).
[14] M.L. Mather, N.R.L. Maccallum, J. Inst. Fuel 40 (May) (1967) 214.
[15] W.G. Rose, in: Trans. ASME 841, J. Appl. Mech. 29 (1962) 615.
[16] R.W. Gore, W.E. Ranz, A.I. Chem. E. J. 10 (1) (1964) 83.
[17] D.G. Lilley, Int. J. Comput. Fluids 4 (1976) 45.
[18] D.G. Lilley, AIAA J. 14 (May (5)) (1976) 547.
[19] V.P. Soldatov, V.V. Kuznetzov, A.A. Morozov, A.A. Kuzakov, A.I. Ovechkin, Inventor's Certificate of USSR No. 969089, 1981.
[20] F.K. Rashidov, A.R. Sakaev, Proceedings of the IV Republican Scientific and Technical Energy Workshop, Tashkent, September, 1973, pp. 108–109.
[21] Yu.N. Kolomiets, Chromatogr. Sorp. Process. 2 (5–6) (2002) 563–574 (in Russian).
[22] A.K. Gupta, D.G. Lilley, N. Syred, Swirl Flows, Abacus Press, 1984, Chapter 1 (Introduction).
[23] Yu.P. Gorbachev, V.V. Ionov, Yu.N. Kolomiets, Russian Patent 2,279,051 (2004).
[24] V.S. Motchkine, L.Y. Krasnobaev, S.N. Bunker, U.S. Patent 6,861,646 (2005).
[25] V.V. Pervukhin, R.R. Ibragimov, V.M. Moralev, Instrum. Exp. Tech. (5) (1997) 122.
[26] V.V. Pervukhin, D.G. Sheven, Tech. Phys. 78 (1) (2008) 114–120.